

*The essential role of Fe(III) ion removal  
over efficient/low-cost activated carbon:  
surface chemistry and adsorption behavior*

**Panya Maneechakr & Surachai  
Karnjanakom**

**Research on Chemical Intermediates**

ISSN 0922-6168

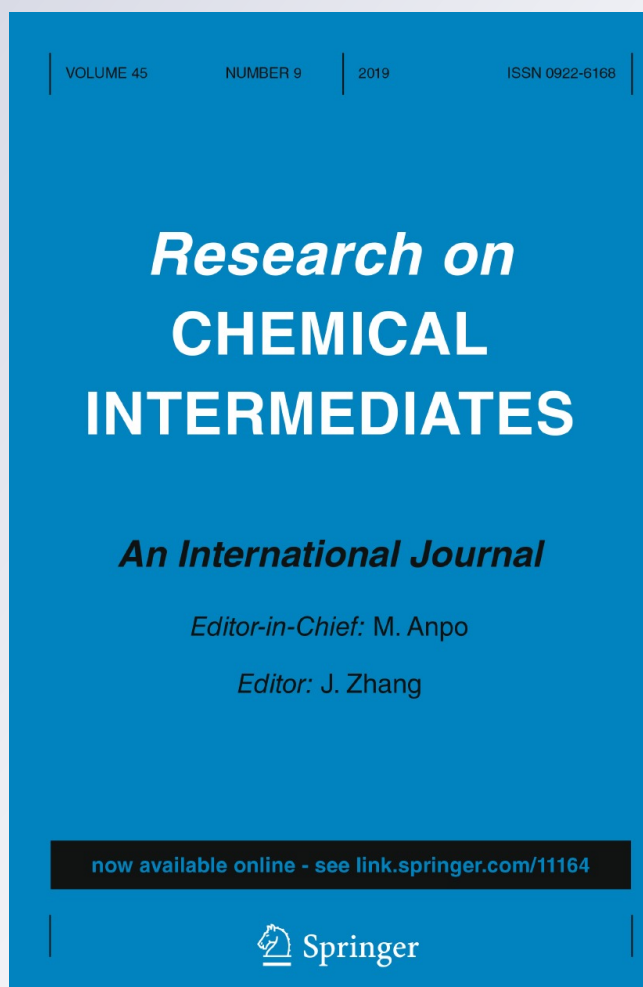
Volume 45

Number 9

Res Chem Intermed (2019)

45:4583-4605

DOI 10.1007/s11164-019-03851-y



**Your article is protected by copyright and all rights are held exclusively by Springer Nature B.V.. This e-offprint is for personal use only and shall not be self-archived in electronic repositories. If you wish to self-archive your article, please use the accepted manuscript version for posting on your own website. You may further deposit the accepted manuscript version in any repository, provided it is only made publicly available 12 months after official publication or later and provided acknowledgement is given to the original source of publication and a link is inserted to the published article on Springer's website. The link must be accompanied by the following text: "The final publication is available at [link.springer.com](http://link.springer.com)".**



# The essential role of Fe(III) ion removal over efficient/low-cost activated carbon: surface chemistry and adsorption behavior

Panya Maneechakr<sup>1</sup> · Surachai Karnjanakom<sup>1</sup>

Received: 22 March 2019 / Accepted: 7 May 2019 / Published online: 14 May 2019  
© Springer Nature B.V. 2019

## Abstract

The efficient/low-cost activated carbons were prepared from inedible fruits such as *Cerbera odollam* Gaertn, *Terminalia catappa*, *Ficus lyrata*, *Couroupita guianensis* Aubl and *Hevea brasiliensis* as well as biochars of *Combretum quadrangulare* and *Leucaena Leucocephala* (LL). The physical and chemical activation processes were applied to improve the Fe<sup>3+</sup> adsorption efficiency. As obtained results, LL heated at 500 °C for 2 h (LL502) exhibited best performance for Fe<sup>3+</sup> adsorption with a  $q_e$  value of Fe<sup>3+</sup> (28.18 mg/g). The physicochemical properties of LL502 such as BET surface area, total acid–base amount and pH<sub>pzc</sub> were 247.3 m<sup>2</sup>/g, 2.2647 meq/g and 8.49, respectively. Moreover, the adsorption behaviors of Fe<sup>3+</sup> onto the surface of LL502 were found to be monolayer, physisorption and rapid adsorption processes which could be confirmed by Langmuir and Dubinin–Radushkevich isotherms and pseudo-second order kinetic models, respectively. Adsorption thermodynamics also indicated that the Fe<sup>3+</sup> adsorption processes were endothermic and spontaneous in nature. In addition, 98% of iron removal from ground/surface water was successfully achieved by using LL502. The quality of ground/surface water was acceptable based on comparison with a water quality standard. This research was as expected since as-prepared low-cost adsorbent could be verily applied in a practical treatment process.

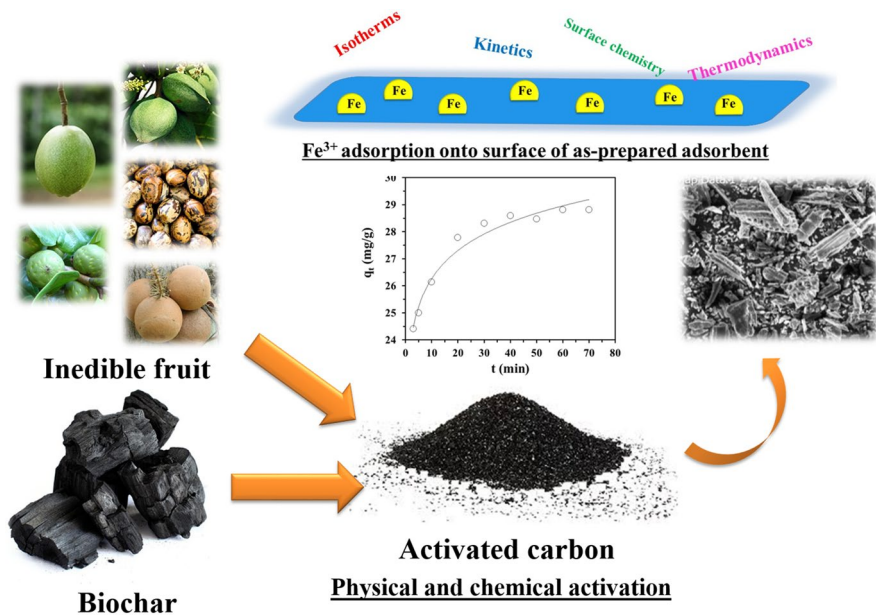
---

✉ Panya Maneechakr  
panya.m@rsu.ac.th

Surachai Karnjanakom  
surachai.ka@rsu.ac.th

<sup>1</sup> Department of Chemistry, Faculty of Science, Rangsit University, Mueang, Pathumthani 12000, Thailand

## Graphical abstract



**Keywords** Iron · Adsorption behavior · Low-cost activated carbon · Inedible fruit · Ground/surface water

## Introduction

Iron (Fe) has been very important for human life because of the demand on formation of red blood cells. The Fe deficiency directly results in anemia while in the case of receiving too much amount of Fe, internal organs of the body such as the liver and pancreas may be destroyed as well. Moreover, Fe has been identified as a toxic metal of environmental concern, which can be easily found in ground/surface water. For industrial processes, the existence or deposition of Fe with a high amount in the water system could lead to several problems such as turbid water, tube failure and slag formation in boilers [1]. In fact, concentration amounts of Fe in ground/surface water should not exceed over 0.5 mg/L which is reported by the U.S. Environmental Protection Agency (EPA) and the World Health Organization (WHO) [2]. Therefore, Fe removal from the environment is a necessary goal, and it should be considered from now on.

Several techniques for removal of metal ions have been reported such as coagulation or co-precipitation by chemical reagents, filtration membranes, ion-exchange and others [3–6]. However, some disadvantages of these techniques are high cost of equipment and chemical, chemical consumption of large amounts, insufficient

removal of metal, complications in large-scale, and they may create residual hazardous by-products. Adsorption procedure has proved to be a reliable/efficient technique for toxic/heavy metal removal from wastewater [7]. Currently, widely used absorbent is activated carbon, which presents cost-effective, high porosity, high degree of surface property and excellent adsorption capability [8]. The increasing or modification of surface area also promotes the metal adsorption performance. Thus, the utilization of activated carbon for Fe removal from wastewater is interesting in current research. In general, the commercial activated carbon (ACC) consisting of high surface area and porosity is used in industrial processes for wastewater treatment. However, considered from the economical point of view, it requires high temperature for pyrolysis and activation procedures, leading to high production cost. Recently, it is found that its excellent performance had been solely limited for adsorptions of non-polar molecules (reactive dye or iodine) and organic compounds (lipids or phenols) while polar molecules including cations and anions are quite low [9]. Based on the abovementioned, it is necessary to develop activated carbon which has high selectivity for the adsorption of metal ions from wastewater.

In this work, efficient/low-cost activated carbons were prepared from two kinds of feedstocks: (I) carbonized carbon derived from inedible fruits such as *Cerbera odollam* Gaertn (COG) *Terminalia catappa* (TC) *Ficus lyrata* (FL) *Couroupita guianensis* Aubl (CGA) and *Hevea brasiliensis* (HB), and (II) biochar of *Combretum quadrangulare* (CQ) and *Leucaena Leucocephala* (LL). It should be noted that these types of carbon feedstocks were selected due to their being abundantly available in Tropical-wet landscapes such as Thailand and other countries [10]. Moreover, they also showed high carbon content and adsorption capacity. The as-prepared adsorbents from the abovementioned were further activated via physical (heating) and chemical ( $H_3PO_4$  and KOH) processes, and also compared with ACC for removal efficiency of  $Fe^{3+}$ . After the activation process, it was expected to expand the amount of carbonyl group on activated carbon with the presence of lone pair electrons which could serve as a Lewis base. Shen et al., 2008 [11] reported the reasonable presence of a carbonyl group with a lone pair electron (Lewis base), leading to well adsorption of metal cations (Lewis acid) via attraction by electrostatic force with the generation of co-ordinate covalent bond. The physical and chemical properties of as-prepared adsorbents such as BET surface area, functional group, acidity-basicity, morphology and  $pH_{pzc}$  were investigated in detail. The adsorption behavior was systematically studied for various factors such as surface chemistry, isotherms, kinetic models, and thermodynamics. This research is expected to obtain high performance low-cost adsorbent for Fe adsorption/removal from aqueous solution including ground/surface water in the environment.

## Experimental

### Materials and reagents

Carbonized carbon derived from inedible fruits such as *Cerbera odollam* Gaertn (COG) *Terminalia catappa* (TC) *Ficus lyrata* (FL) *Couroupita guianensis* Aubl

(CGA) and *Hevea brasiliensis* (HB), and biochar of *Combretum quadrangulare* (CQ) and *Leucaena Leucocephala* (LL) were collected in Thailand and utilized as adsorbent feedstocks for production of activated carbon. Proximate analysis was performed to determine the moisture, ash, volatile matter and fixed carbon of each feedstock using ASTM D2867-95, D2866-94. Commercial activated carbon (ACC) was purchased from Sigma Aldrich (Fluka 05120). All chemical reagents used were of analytical grade and purchased from Merck and Sigma Aldrich Companies.  $\text{FeCl}_3 \cdot 6\text{H}_2\text{O}$  and  $\text{I}_2$  solutions were prepared at concentrations of 130 mg/L and 0.2 mol/L, respectively.

## Preparation of low cost-adsorbent

### Study of the optimum temperature

The inedible fruits placed in confined containers were heated at 400, 450 and 500 °C for 1–3 h under the atmosphere. Then, they were crushed and sieved through a 400 mesh sieve before the adsorption procedure. Here, for instance, carbonized carbons obtained from the carbonization process of COG, TC, FL and CGA at 400 °C for 1 h were denoted as COG-401, TC-401, FL-401 and CGA-401, respectively. For biochar of CQ and LL, they were also crushed and sieved through a 400 mesh sieve at first, and then heated at 500 °C for 1–5 h. Here, for instance, carbonized carbons obtained from the carbonization process of CQ and LL biochar at 500 °C for 1 h were denoted as CQ-501 and LL-501, respectively.

### Study of the chemical activation process

The 3 g of selected carbonized carbon was mixed with 30%w/w of  $\text{H}_3\text{PO}_4$  solution or KOH pellet at different weight ratios of carbonized carbon to  $\text{H}_3\text{PO}_4$  or KOH such as 1:2, 1:3, 1:4 and 1:5, and then activated at 400, 450 and 500 °C for 1–3 h. Finally, the obtained samples were washed with distilled water until neutral pH. Here, for instance, activated carbons obtained from chemical ( $\text{H}_3\text{PO}_4$  and KOH) activation processes at 400 °C for 1 h were denoted as ACP-401 and ACK-401, respectively.

## Adsorbent characterization

### Surface area, morphology and element

The surface area of as-prepared adsorbent was measured by using a Quantachrome instrument (NOVA 4200e, USA) at liquid  $\text{N}_2$  temperature of  $-196$  °C using the Brunauer–Emmett–Teller (BET) method. Before  $\text{N}_2$  sorption analysis, all samples were degassed at 150 °C for 4 h. The adsorbent morphology and the existence of absorbed metal species such as Fe on adsorbent were observed using a scanning electron microscope (SEM S-4800; Hitachi) equipped with an energy dispersive spectroscopy (EDS). Before the SEM observation, the dried sample was dispersed on carbon tape supported on a stub and then pretreated by Pt sputtering.

## Surface functional group and total acidity-basicity

The presence of each functional group on the surface of prepared adsorbent was verified by Fourier transform infrared spectrometry (FT-IR) using a PerkinElmer Spectrum 100 FT-IR spectrometer in the range of wavenumber between 4000 and 500  $\text{cm}^{-1}$ . The amounts of acidic and basic functional groups on adsorbent were determined by the Boehm titration method [12]. In brief, to quantify the amount of carboxylic, lactone and phenolic groups, 0.5 g of adsorbent was added into 25 mL of 0.1 mol/L NaOH, 0.1 mol/L  $\text{Na}_2\text{CO}_3$  and 0.1 mol/L  $\text{NaHCO}_3$  solutions. Then, it was stirred at a speed of 150 rpm with a temperature of 30 °C for 24 h, and titrated with 0.1 mol/L HCl solution. For the basicity test, the adsorbent was added into 25 mL of 0.1 mol/L HCl solution and then titrated with 0.1 mol/L NaOH solution.

## Determination of point of zero charge ( $\text{pH}_{\text{pzc}}$ )

A total of 0.1 g of adsorbent was added into 25 mL of 0.1 mol/L NaCl and then pH was adjusted to remain within the range between 1 and 9 [13]. The mixture solution was stirred at a temperature of 303.15 K for 30 min with a speed of 150 rpm. After complete stirring, the mixture solution was measured for surface charges by a pH Eutech instrument, pH 7.00 with the uncertainty of  $\pm 0.1$ .

## Adsorption studies

All the adsorbents prepared from the abovementioned were syntactically investigated to find the optimum conditions for  $\text{Fe}^{3+}$  adsorptions before further studies on isotherms, kinetic models and thermodynamic adsorptions. In a typical procedure, 0.1 g of adsorbent was added into 25 mL of 130 mg/L  $\text{Fe}^{3+}$  and stirred at a speed of 150 rpm with a temperature of 303.15 K for 30 min. Meanwhile, the study on adsorption of 0.05 mol/L  $\text{I}_2$  was also performed under the same conditions with the  $\text{Fe}^{3+}$  adsorption process. After the finishing procedure, adsorbents were separated by filtration, and the obtained solutions were then analyzed to find the remaining concentrations of  $\text{Fe}^{3+}$  and  $\text{I}_2$ . The concentrations of  $\text{Fe}^{3+}$  were analyzed using a 1, 10-Phenanthroline method on a UV-Visible spectrophotometer at a wavelength of 510 nm (Genesys 20) while  $\text{I}_2$  concentration was determined by titration with  $\text{S}_2\text{O}_3^{2-}$  solutions. The amount of adsorption at equilibrium ( $q_e$ ,  $\text{mg g}^{-1}$ ) was calculated according to Eq. (1) [14]:

$$q_e = \frac{(C_0 - C_e)V}{M}, \quad (1)$$

where  $C_e$  is the equilibrium concentration of the  $\text{Fe}^{3+}$  (mg/L),  $C_0$  is the initial concentration of  $\text{Fe}^{3+}$  (mg/L),  $V$  is the volume of the solution (L) and  $M$  is the mass of adsorbent (g).

The details of adsorption isotherms, kinetics and thermodynamics are provided in Figs. 3, 4, 5 and Table 7.

### Qualitative analysis of ground/surface water before and after adsorption processes

The 4 g of LL502 was added into 500 mL of ground water or surface water and stirred at a speed of 150 rpm with a temperature of 303.15 K for 60 min. It should be noted that ground/surface water samples were collected in Bangkok, Thailand. After finishing process, LL502 were separated by filtration and the obtained solutions were then analyzed to find the remaining concentrations of  $\text{Fe}^{3+}$  including water quality indicators such as pH, hardness and  $\text{Cl}^-$  using Standard Methods for the Examination of Water and Wastewater 18<sup>th</sup> Edition 1992.

## Results and discussion

### Effect of physical activation for production of carbonized carbon and activated carbon

Table 1 shows the results of proximate analysis of each inedible fruit. One can see that all kinds of inedible fruits had high volatile matter contents, indicating the presence of organic substances in high amounts that could be easily decomposed at high temperature. Also, the percentages of fixed carbons and moistures derived from all samples were not so much different. Considering on semblance of all samples, TC and FL had the same feature (soft outer shell/hard inner shell), which was contrasted with HB (hard outer shell/soft inner shell). For COG and CGA, they had bigger shape than other samples. Table 2 shows characteristics of each adsorbent physically activated at 400–500 °C for 1–3 h based on  $\text{I}_2$  and  $\text{Fe}^{3+}$  adsorptions. It should be mentioned here that  $\text{I}_2$  was also applied as an adsorbate in this study in order to check the polarity on the surface of as-prepared adsorbent. One can see that TC501 had maximum values of  $\text{I}_2$  adsorption (552.93 mg/g) and  $\text{Fe}^{3+}$  adsorption (23.67 mg/g), and followed by COG501 at the amounts of  $\text{I}_2$  adsorption (537.22 mg/g) and  $\text{Fe}^{3+}$  adsorption (21.25 mg/g). In the case of biochar (CQ and LL), as shown in Table 3, CQ exhibited lower adsorption capacities of  $\text{I}_2$  and  $\text{Fe}^{3+}$  than LL, probably due to the existence of carbon composition with higher tightness.

**Table 1** Proximate analysis of various kinds of inedible fruits

Proximate analysis (wt%)	COG	TC	FL	CGA	HB
Moisture	18.88	17.25	17.35	18.75	15.25
Ash	4.65	3.46	3.55	4.23	2.76
Volatile matter	50.83	59.65	59.1	52.87	63.74
Fixed carbon <sup>a</sup>	25.64	19.64	20.00	24.15	18.25

<sup>a</sup>Fixed carbon was determined from mass difference

**Table 2** The efficiencies of carbonized carbons derived from carbonization of various kinds of inedible fruits at 400–500 °C for 1–3 h for I<sub>2</sub> and Fe<sup>3+</sup> adsorption

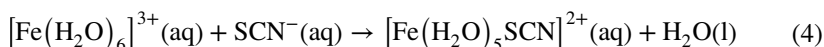
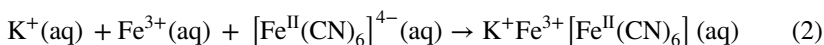
Adsorbent	I <sub>2</sub> No. (mg/g)	q <sub>e</sub> of Fe <sup>3+</sup> (mg/g)	Adsorbent	I <sub>2</sub> No. (mg/g)	q <sub>e</sub> of Fe <sup>3+</sup> (mg/g)	Adsorbent	I <sub>2</sub> No. (mg/g)	q <sub>e</sub> of Fe <sup>3+</sup> (mg/g)	Adsorbent	I <sub>2</sub> No. (mg/g)	q <sub>e</sub> of Fe <sup>3+</sup> (mg/g)	Adsorbent	I <sub>2</sub> No. (mg/g)	q <sub>e</sub> of Fe <sup>3+</sup> (mg/g)
COG	316.33	12.65	TC	262.49	13.42	FL	295.14	10.52	CGA	222.56	7.95	HB	200.17	8.69
COG401	418.34	14.26	TC401	498.63	15.65	FL401	442.31	12.26	CGA401	420.91	12.63	HB401	390.54	15.65
COG402	406.92	15.35	TC402	508.65	16.55	FL402	439.26	13.57	CGA402	404.37	15.65	HB402	377.05	14.23
COG403	283.11	16.45	TC403	514.35	17.21	FL403	491.12	15.55	CGA403	443.64	16.66	HB403	380.95	13.99
COG451	420.35	17.12	TC451	491.49	18.21	FL451	398.25	14.11	CGA451	398.33	15.23	HB451	401.25	16.12
COG452	452.67	17.65	TC452	517.92	18.50	FL452	388.14	14.23	CGA452	375.56	15.04	HB452	410.56	16.56
COG453	444.17	18.01	TC453	502.92	18.96	FL453	355.12	14.65	CGA453	366.99	15.35	HB453	406.23	16.55
COG501	537.22	21.25	TC501	552.93	23.67	FL501	298.94	13.33	CGA501	372.09	14.22	HB501	438.54	17.36
COG502	491.74	21.12	TC502	514.35	22.65	FL502	262.33	13.65	CGA502	386.59	14.36	HB502	469.44	18.26
COG503	409.65	20.35	TC503	461.49	22.55	FL503	283.69	13.45	CGA503	372.96	13.99	HB503	465.56	18.11
Precision	<±2.17	<±0.67	–	<±3.56	<±0.58	–	<±4.23	<±0.74	–	<±3.38	<±0.89	–	<±4.44	<±0.62

(n = 3, α = 0.95)

**Table 3** The efficiencies of carbonized carbons derived from carbonization of various kinds of biochar (CQ and LL) at 500 °C for 1–5 h for I<sub>2</sub> and Fe<sup>3+</sup> adsorptions

Adsorbent	Burn loss (%)	I <sub>2</sub> No. (mg/g)	q <sub>e</sub> of Fe <sup>3+</sup> (mg/g)	Adsorbent	Burn loss (%)	I <sub>2</sub> No. (mg/g)	q <sub>e</sub> of Fe <sup>3+</sup> (mg/g)
CQ	–	307.82 ± 1.25	15.61 ± 0.85	LL	–	484.17 ± 0.21	25.32 ± 0.22
CQ501	15.22	380.01 ± 2.25	20.23 ± 0.65	LL501	18.60	498.76 ± 0.08	25.60 ± 0.21
CQ502	20.45	397.98 ± 2.03	20.15 ± 0.55	LL502	21.17	505.69 ± 0.07	28.18 ± 0.23
CQ503	22.33	580.33 ± 3.25	21.01 ± 0.47	LL503	23.39	561.39 ± 0.15	28.91 ± 0.19
CQ504	23.35	590.56 ± 1.78	20.47 ± 0.65	LL504	25.00	512.17 ± 0.22	28.35 ± 0.19
CQ505	24.67	535.88 ± 1.56	19.35 ± 0.56	LL505	29.20	500.55 ± 0.19	28.04 ± 0.18
ACC	–	1057.55 ± 0.11	11.93 ± 0.25	–	< ± 1.78	< ± 0.22	< ± 0.23
Precision ( <i>n</i> = 3, <i>α</i> = 0.95)	< ± 1.25	< ± 3.25	< ± 0.85	–			

Here, tightness values calculated from CQ and LL powders were 0.47 and 0.42 g/mL, respectively. Considering on break-even point, the weight loss in a sample was obviously decreased to some extent with an increase in the activation time, resulting in the increasing of adsorption performance. As expected, the maximum values of  $I_2$  adsorption (561.39 mg/g) and  $Fe^{3+}$  adsorption (28.91 mg/g) were found for LL503. However, in order to save energy for the activation process, LL502 was selected to replace LL503 since their adsorption capacities of  $Fe^{3+}$  were a small difference. After finishing adsorption processes, all filtrates were tested by  $SCN^-$  with  $[Fe^{III}(CN)_6]^{3-}$  solutions. One can see that the blue color of  $Fe^{3+}[Fe^{II}(CN)_6]^-$  solution clearly appeared as in Eqs. (2) and (3), indicating that  $Fe^{3+}$  could be reduced into  $Fe^{2+}$  [9]. Meanwhile,  $Fe^{3+}$  could also serve as an oxidizing agent for increasing the oxygen groups on the surface of adsorbent. It should be noted that no red color of  $Fe(SCN)^{2+}$  solution was found for all filtrates as in Eq. (4).



Interestingly, as shown in Table 3, ACC presented the highest  $I_2$  adsorption capacity (1057.55 mg/g) when compared with other samples, resulting from its highest surface area and porosity. Unfortunately, a lowest  $Fe^{3+}$  adsorption capacity (11.93 mg/g) was obtained obviously. This phenomenon could be attributed to lower polarity on the surface of ACC than the biochar activated at 500 °C for 1–5 h. From these results, TC501 and LL502 were selected for further study.

### Effect of chemical activation by $H_3PO_4$ and KOH

Table 4 shows characteristics of each adsorbent chemically activated at 400–500 °C for 1–3 h based on  $I_2$  and  $Fe^{3+}$  adsorptions. For activation by  $H_3PO_4$ , TC501- $H_3PO_4$  chemically activated at all conditions exhibited  $I_2$  and  $Fe^{3+}$  adsorption capacities in the range of 501.93–560.89 mg/g and 21.03–24.66 mg/g, respectively, which had no significant difference, comparing to TC501 ( $I_2=552.93$  mg/g) and ( $Fe^{3+}=23.67$  mg/g) in Tables 2 and 3. In the case of LL502- $H_3PO_4$  chemically activated at 400 °C for 3 h with weight ratios of adsorbent to  $H_3PO_4$  (1:5), higher adsorption capacities of  $I_2$  (752 mg/g) and  $Fe^{3+}$  (28.35 mg/g) were obtained when compared with LL502 ( $I_2=505.69$  mg/g and  $Fe^{3+}=28.18$  mg/g). For activation by KOH, one can see that lower efficiency for  $I_2$  adsorption was found for TC501-KOH chemically activated at all conditions when compared with TC501. In this study, a maximum adsorption capacity (28.55 mg/g) for  $Fe^{3+}$  was also obtained using LL502-KOH chemically activated at 500 °C for 1 h with weight ratios of adsorbent to KOH (1:5). Based on above results, even though the chemical activation by  $H_3PO_4$  and KOH resulted in improving the  $I_2$  and  $Fe^{3+}$  adsorption efficiencies, they were not so suitable since a few of increasing capacity were obtained in this study.

**Table 4** The efficiencies of activated carbon derived from activation of various kinds of carbonized carbons (TC-501 and LL-502) at 400–500 °C for 1–3 h for I<sub>2</sub> and Fe<sup>3+</sup> adsorptions

Temperature (°C)	Time (min)	Ratio of adsorbent to H <sub>3</sub> PO <sub>4</sub> or KOH		I <sub>2</sub> No. (mg/g)				q <sub>e</sub> of Fe <sup>3+</sup> (mg/g)			
				TC501		LL502		TC501		LL502	
		H <sub>3</sub> PO <sub>4</sub>	KOH	H <sub>3</sub> PO <sub>4</sub>	KOH	H <sub>3</sub> PO <sub>4</sub>	KOH	H <sub>3</sub> PO <sub>4</sub>	KOH	H <sub>3</sub> PO <sub>4</sub>	KOH
400	60	1:2	474.13	373.54	465.68	23.12	24.00	26.25	27.15		
		1:3	449.50	508.40	453.66	23.01	24.12	25.25	27.36		
		1:4	440.26	641.08	474.69	22.98	24.06	25.17	27.44		
		1:5	437.18	678.05	429.63	22.65	23.65	24.15	27.54		
		1:2	474.13	425.75	462.68	23.00	24.69	26.22	27.36		
400	120	1:2	486.44	645.43	483.71	22.95	24.78	25.36	27.10		
		1:3	492.60	625.85	468.68	22.54	24.00	25.68	27.65		
		1:4	449.50	699.80	438.64	22.32	24.12	25.35	27.00		
		1:5	477.20	449.67	465.68	21.65	23.69	27.35	27.36		
		1:2	498.76	630.20	450.66	21.85	23.71	27.65	27.65		
400	180	1:3	467.97	725.90	405.59	21.65	23.89	28.00	27.01		
		1:4	406.39	752.00	363.53	21.03	22.96	28.35	27.11		

**Table 4** (continued)

Temperature (°C)	Time (min)	Ratio of adsorbent to H <sub>3</sub> PO <sub>4</sub> or KOH	I <sub>2</sub> No. (mg/g)		q <sub>e</sub> of Fe <sup>3+</sup> (mg/g)					
			TC501 H <sub>3</sub> PO <sub>4</sub>	TC501 KOH	LL502 H <sub>3</sub> PO <sub>4</sub>	LL502 KOH	TC501 H <sub>3</sub> PO <sub>4</sub>	TC501 KOH	LL502 H <sub>3</sub> PO <sub>4</sub>	LL502 KOH
500	60	1:2	525.84	449.50	353.97	408.60	24.36	25.01	28.15	28.55
		1:3	538.58	517.23	523.62	465.68	24.15	25.12	28.23	28.45
		1:4	554.52	486.44	643.25	498.73	24.00	24.99	27.23	27.65
		1:5	559.30	495.68	708.50	492.72	24.66	24.85	27.55	26.52
		1:2	508.31	409.47	417.05	333.49	24.12	24.36	26.98	26.22
120	120	1:3	548.14	538.78	534.50	522.78	24.03	24.65	25.21	26.23
		1:4	551.33	541.86	634.55	474.69	24.00	25.03	25.99	26.87
		1:5	560.89	529.54	671.53	513.75	24.00	25.00	25.65	26.84
		1:2	514.68	511.07	390.95	405.59	23.35	24.36	26.12	25.65
		1:3	540.18	548.02	477.95	522.76	23.25	24.12	26.23	25.36
180	180	1:4	560.89	535.70	645.43	480.70	23.32	24.37	25.98	25.55
		1:5	557.70	530.16	669.35	528.77	23.33	23.66	25.23	24.98

Moreover, it required large amounts of water for washing of acid–base during activation process. Therefore, LL502 without chemical activation was selected for further study. It should be noted that unsuitable conditions for the chemical activation process occurred, as, for instance, surface/porous structure of activated carbon was destroyed when too much acid or base might be applied.

### Properties of as-prepared adsorbent

To confirm the adsorption behavior/efficiency of  $\text{Fe}^{3+}$  onto adsorbent, functional groups,  $\text{pH}_{\text{pzc}}$  values and textural properties were investigated, and the results are shown in Table 5. Here, the total functional groups of each adsorbent were in the order of LL-502-  $\text{H}_3\text{PO}_4$  > LL-502 > LL > ACC. As observed, total acid amount was higher than total basic amount which corresponded to  $\text{pH}_{\text{pzc}}$  value of ACC (<7), indicating that the surface of ACC had acid properties. In contrast, according to  $\text{pH}_{\text{pzc}}$  value of LL (>7), its surface had basic properties based on total acid (0.5635 meq/g) and base (1.3640 meq/g) amounts. Interestingly, for LL502 and LL502- $\text{H}_3\text{PO}_4$ , carboxylic and phenolic groups were reduced to some extent by converting into  $\text{CO}_2$  while a lactone group occurred from structural rearrangement from the hydroxyl group into the carbonyl group and total acid-basic amounts were obviously increased, comparing with LL to without activation process [15]. This may be one reason for promoting the  $\text{Fe}^{3+}$  adsorption efficiency by increasing the lactone group. Moreover, one can see that all adsorbents presented values of  $\text{pH}_{\text{pzc}}$  (5.55–8.49) > pH of  $\text{Fe}^{3+}$  (in the mixture solution of  $\text{Fe}^{3+}$  and adsorbent), indicating that the adsorbent surface was well predominated by negative charge, leading to a possibility for  $\text{Fe}^{3+}$  adsorption. In addition, LL-502 had the highest  $\text{pH}_{\text{pzc}}$  value of 8.49 while the lowest  $\text{pH}_{\text{pzc}}$  value of 5.55 was found for ACC, resulting in better  $\text{Fe}^{3+}$  adsorption ability for LL-502.

As shown in Table 5, the surface area was evidently increased after LL was activated, resulting in the increasing of  $\text{Fe}^{3+}$  adsorption ability. In the case of ACC, even though it had much higher surface area than the other one,  $\text{Fe}^{3+}$  adsorption ability was very low, resulting from the presence of lower total acid-basic amounts. Figure 1 shows FT-IR spectra results of as-prepared adsorbents. It is found that the bands at wavenumbers of 3500, 2900, 1650, 1030  $\text{cm}^{-1}$  clearly appeared for all adsorbents which could be attributed to the vibrations of  $-\text{OH}$ ,  $\text{N}-\text{H}/\text{C}-\text{H}$ ,  $\text{C}=\text{O}$  and  $\text{C}-\text{O}$ , respectively [16–18]. As observed, the higher intensity peak of  $\text{C}=\text{O}$  derived from LL502 was found when compared with other one, especially for ACC, leading to better  $\text{Fe}^{3+}$  adsorption efficiency. Figure 2 shows the SEM–EDS result of LL502 after  $\text{Fe}^{3+}$  adsorption. As expected, iron species were well adsorbed with homogeneous dispersion on the surface of LL502.

### Qualities of ground/surface water

Table 6 shows the analysis results of ground/surface water before and after the adsorption process using LL502. It is found that values of pH, hardness and  $\text{Cl}^-$  subsisted in ground/surface water, except for Fe content, and did not exceed the water quality

**Table 5** Surface chemical and textural properties of as-prepared adsorbents

Adsorbent	Surface area (m <sup>2</sup> /g)	Pore size (nm)	Amount of functional group (meq/g)				Total acidic and basic	pH <sub>pzc</sub>	pH in Fe <sup>3+</sup>	
			Carboxylic	Lactone	Phenolic	Total acidic				Total basic
ACC	901.14	5.55	0.0343	0.0643	0.6043	0.7029	0.4522	1.1551	5.55	2.75
LL	86.9	2.99	0.0112	0.0834	0.4686	0.5635	1.3640	1.7191	8.29	2.98
LL-502	247.3	3.96	0.0075	0.2222	0.4088	0.6385	1.6262	2.2647	8.49	3.27
ACPLL-502	262.1	2.97	0.0073	0.2388	0.3791	0.6252	1.7645	2.3897	5.65	3.03

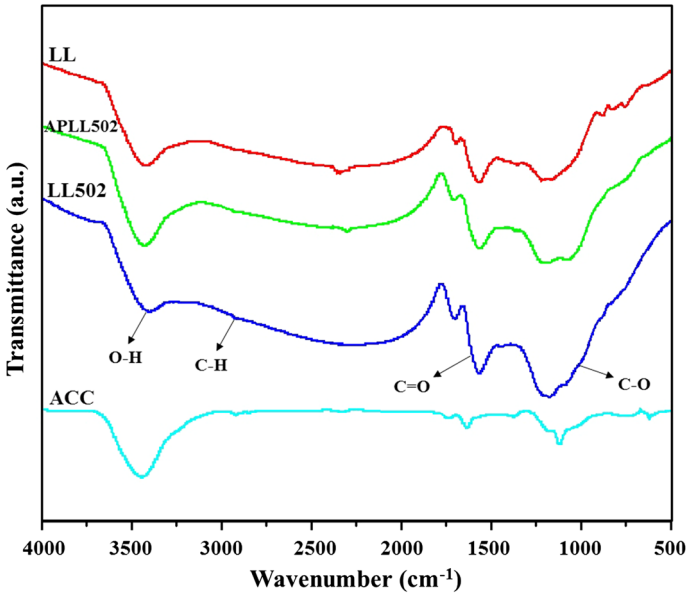


Fig. 1 FT-IR spectra of various adsorbents

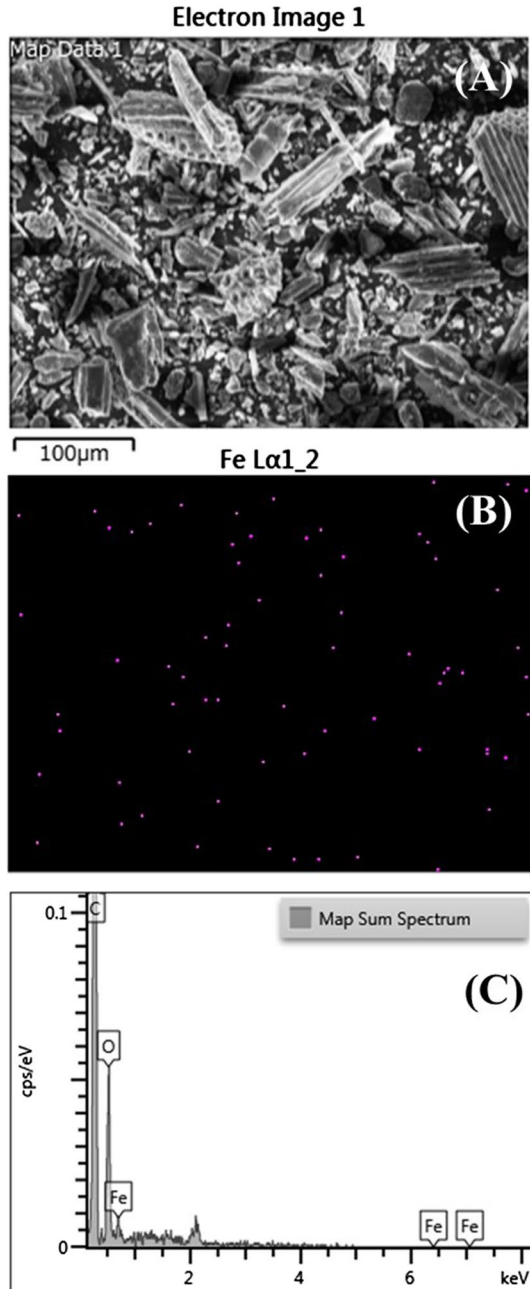
standard. After treatment by the adsorption process, Fe content in ground/surface water was decreased from 2.5 mg/L into 0.05 mg/L (98% of Fe removal in ground water) and from 2.0 mg/L into 0.05 mg/L (98% of Fe removal in surface water), which were passable values in water quality standards. Moreover, the hardness value also decreased significantly. In addition,  $\text{Cl}^-$  content was slightly decreased after the treatment process, suggesting that the surface of LL502 had  $\text{pH}_{\text{pzc}} > \text{pH}$  of ground/surface water. This result could be also verified so that the existence of negative charge on the LL502 surface promoted adsorptions of metal cations including  $\text{Fe}^{3+}$ , while its efficiency for adsorption of  $\text{Cl}^-$  anion was low in this study.

### Adsorption isotherm, kinetic and thermodynamic

Studying the adsorption behaviour was simulated by the equilibrium isotherms of Langmuir, Freundlich, and Dubinin–Radushkevich based on varying concentrations of  $\text{Fe}^{3+}$  solution (Fig. 3). For the Langmuir isotherm model, it was applied to point out the assumption of monolayer adsorption onto a surface containing a finite number of adsorption sites without interaction between adsorbed molecules on neighboring sites and transmigration of adsorbate in the plane of the surface [19]. The linear model of Langmuir isotherm is provided by the following Eq. (5):

$$\frac{C_e}{q_e} = \frac{1}{q_{\text{max}}K} + \frac{1}{q_{\text{max}}}C_e, \quad (5)$$

**Fig. 2** **a** SEM image, **b** EDS mapping and **c** EDS spectrum of LL502 after  $\text{Fe}^{3+}$  adsorption



where  $C_e$  is the equilibrium concentration of the  $\text{Fe}^{3+}$  (mg/L),  $q_e$  is the amount of adsorption at equilibrium (mg/g),  $q_{\max}$  is the Langmuir maximum adsorption capacity of  $\text{Fe}^{3+}$  per unit mass of LL502 (mg/g) and  $K$  is the Langmuir constant related to the adsorption equilibrium (L/mg).

**Table 6** The data of water quality index for ground/surface water before and after treatment using LL502

Water quality index	Ground water		Surface water		Water quality standard	
	Before treatment	After treatment	Before treatment	After treatment	Appropriate criteria	Maximum threshold
pH	7.04	7.15	7.11	7.10	7.0–8.5	6.5–9.2
Hardness (mg CaCO <sub>3</sub> /L)	250	50	82	50	< 300	500
Cl <sup>-</sup> (mg/L)	95	88	70	77	< 250	600
Fe (mg/L)	2.5	0.05	2.0	0.05	< 0.5	1.0

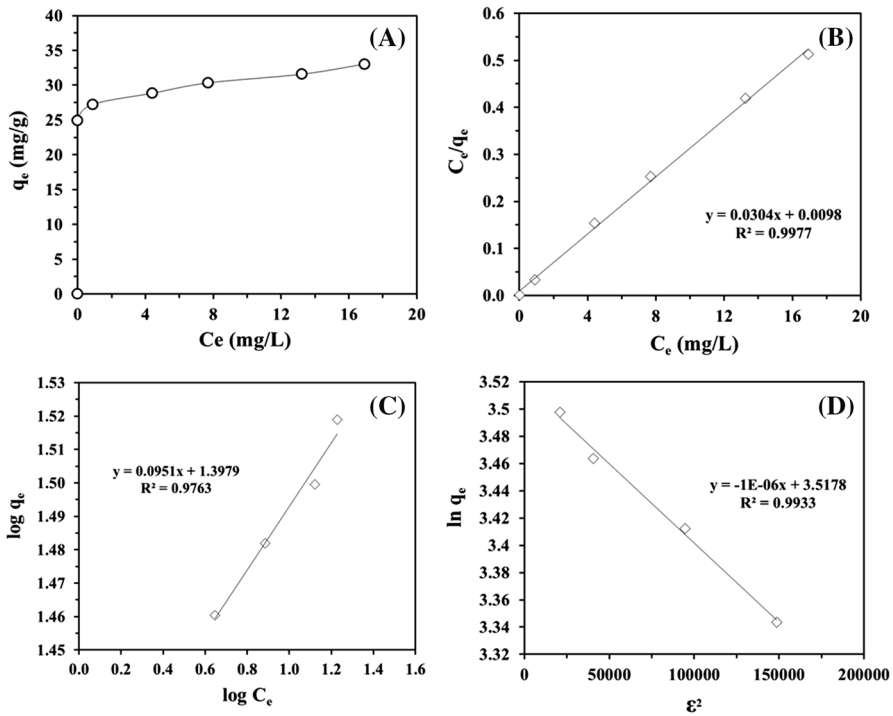


**Fig. 3** **a** Equilibrium adsorption, **b** Langmuir, **c** Freundlich and Dubinin–Radushkevich adsorption isotherm of  $Fe^{3+}$  onto LL502. Relative combined expanded uncertainty  $tSE$  is  $\pm 0.03$  mg/g (0.95 level of confidence). The initial concentration of adsorbate ( $C_0$ ) of  $Fe^{3+}$  = 90–140 mg/L 25 mL, adsorbent = 0.1 g, time ( $t$ ) = 30 min and temperature ( $T$ ) = 303.15 K

For Freundlich isotherm model, it was applied to point out the assumption of multilayer/physical adsorption with non-uniform distribution of heat over heterogeneous surface of adsorbent [20]. The linear model of a Freundlich isotherm is provided by the following Eq. (6):

$$\log q_e = \log K_F + \frac{1}{n} \log C_e, \tag{6}$$

where  $K_F$  is the Freundlich constant related to the adsorption capacity (mg/g/(mg)<sup>1/n</sup>) and  $n$  is the intensity of adsorption and constants incorporating the factors affecting the adsorption capacity.

For the Dubinin–Radushkevich model, it was applied to define the adsorption mechanism and nature based on porosity attendance free energy [21]. The linear model of the Dubinin–Radushkevich isotherm is provided by the following Eq. (7):

$$\ln q_e = \ln q_s - B\epsilon^2, \tag{7}$$

where  $q_s$  is the theoretical saturation capacity (mg/g),  $B$  is the Dubinin–Radushkevich constant related to biosorption energy (mol<sup>2</sup>/kJ) and  $\epsilon$  is the Polanyi potential which can be calculated by the following Eq. (8):

$$\varepsilon = RT \ln \left( 1 + \frac{1}{C_e} \right). \quad (8)$$

Meanwhile, the free energy of adsorption ( $E$ , kJ/mol) was also calculated by the following Eq. (9):

$$E = \frac{1}{\sqrt{2B}}. \quad (9)$$

Here, the magnitude of  $E$  might useful for estimating the mechanism of the adsorption reaction. It should be mentioned here that the physical force and ion exchange mechanism may affect the adsorption mechanisms at  $E < 8$  kJ/mol and  $E = 8$ –16 kJ/mol, respectively.

Figure 3b–d and Table 7 shows the equilibrium isotherms determined from linear models for  $\text{Fe}^{3+}$  adsorption using LL502 at mild conditions. Considering the  $R^2$  value, the adsorption results were well-fitted with the Langmuir isotherm ( $R^2 > 0.99$ ) and also found to be greater than that of the Freundlich isotherm ( $R^2 = 0.9763$ ), indicating monolayer adsorptions of  $\text{Fe}^{3+}$  (Lewis acid/positive charge) onto the LL502 surface (with the existence of a lone pair electrons/Lewis base derived from a total functional group as well as negative charge based on  $\text{pH}_{\text{pzc}} > 7$ ) via electrostatic force with the generation of a co-ordinate covalent bond. Here, a  $q_{\text{max}}$  value obtained from  $\text{Fe}^{3+}$ , adsorption using LL502 was 32.89 mg/g. For the Dubinin–Radushkevich isotherm, it could be also considered since its  $R^2$  value ( $> 0.99$ ) was obtained. Also, its  $E$  value of  $\text{Fe}^{3+}$  adsorption was 0.6561 kJ/mol which was lower than 8 kJ/mol, corresponding to physical adsorption [22]. Meanwhile,  $q_s$  value calculated from the Dubinin–Radushkevich isotherm (33.71 mg/g) was rather close to the  $q_{\text{max}}$  value calculated from the Langmuir isotherm (32.89 mg/g), indicating the accuracy of the applied model via the monolayer-physisorption process.

In order to describe this in terms of adsorption rate, the kinetic study of  $\text{Fe}^{3+}$  adsorption on LL502 was simulated with linear equations of pseudo-first order and pseudo-second order which were given by the following Eqs. (10) and (11), respectively [23, 24]:

$$\log (q_e - q_t) = \log q_e - \frac{k_1}{2.303} t, \quad (10)$$

$$\frac{t}{q_t} = \frac{1}{k_2 q_e^2} + \frac{1}{q_e} t, \quad (11)$$

where  $q_e$  and  $q_t$  (mg/g) are the amount of  $\text{Fe}^{3+}$  at equilibrium and at any time, respectively.  $k_1$  and  $k_2$  are the pseudo-first order and the pseudo-second order rate constants, respectively.  $t$  is the contact time (min).

Figure 4a show the adsorption performance of  $\text{Fe}^{3+}$  onto LL502 at different contact times. Here, a rapid initiative adsorption was started at a contact time of 3 min, then gradually increased and became close to equilibrium within 30 min. This phenomenon might be explained on the existence many adsorption sites with adequate vacant sites in

**Table 7** Isotherm, kinetic and thermodynamic parameters and their correlation coefficients for Fe<sup>3+</sup> adsorption using LL502

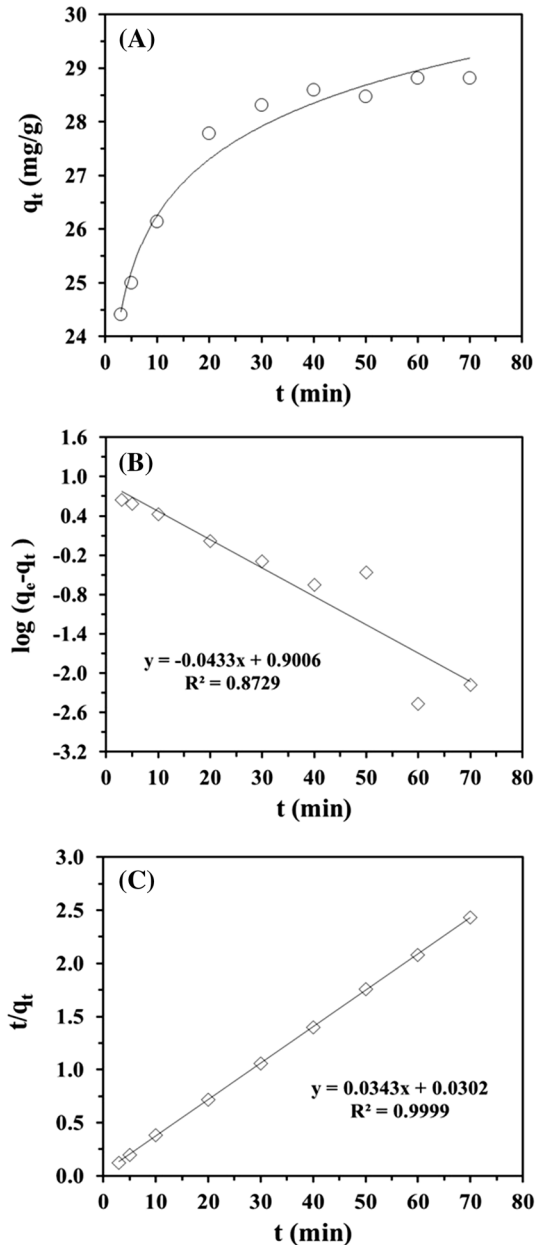
Adsorbent	Langmuir parameters			Freundlich parameters			Dubinin–Radushkevich parameters			
	$q_{max}$ (mg/g)	$K_L$ (L/mg)	$R^2$	$1/n$	$K_F$	$R^2$	$q_s$ (mg/g)	$B$ (mol <sup>2</sup> /kJ)	$E$ (kJ/mol)	$R^2$
LL502	Adsorption equilibrium <sup>a</sup>									
	32.89	3.11	0.9977	0.0951	25.00	0.9763	33.71	1.16	0.6561	0.9933
Adsorption kinetic <sup>b</sup>										
$q_e$ exp (mg/g)	Pseudo-first-order			Pseudo-second-order						
	$q_e$ cal	$k_1$	$R^2$	$q_e$ cal	$k_2$	$R^2$				
28.82	7.95	0.100	0.8729	29.15	0.039	0.9999				
Adsorption thermodynamic <sup>c</sup>										
$\Delta H$ (KJ/mol)	$\Delta S$ (J/molK)	$\Delta G$ (KJ/mol)								
54.59	208.02	303.15 K	313.15 K	323.15 K	328.15 K	$R^2$				
		-8.50	-10.38	-12.65	-13.65	0.9977				

<sup>a</sup>The initial concentration of adsorbate ( $C_0$ ) of Fe<sup>3+</sup> = 90–140 mg/L, 25 mL, adsorbent = 0.10 g, time ( $t$ ) = 30 min and temperature ( $T$ ) = 303.15 K

<sup>b</sup>The initial concentration of adsorbate ( $C_0$ ) of Fe<sup>3+</sup> = 120 mg/L, 25 mL, adsorbent = 0.10 g, time ( $t$ ) = 3–70 min and temperature ( $T$ ) = 303.15 K

<sup>c</sup>The initial concentration of adsorbate ( $C_0$ ) of Fe<sup>3+</sup> = 120 mg/L, 25 mL, adsorbent = 0.10 g, time ( $t$ ) = 60 min and temperature ( $T$ ) = 303.15–328.15 K

**Fig. 4** **a** Effect of contact time, **b** Pseudo-first-order and **c** Pseudo-second-order kinetics of  $\text{Fe}^{3+}$  adsorption onto LL502. Relative combined expanded uncertainty tSE is  $\pm 0.02$  mg/g (0.95 level of confidence). The initial concentration of adsorbate ( $C_0$ ) of  $\text{Fe}^{3+}$  = 120 mg/L, 25 mL, adsorbent = 0.10 g, time ( $t$ ) = 3–70 min and temperature ( $T$ ) = 303.15 K



the inception phase. In addition, the saturation points of absorption sites of LL502 were well reached at the time extended. To obtain more details on adsorption rate, as shown in Fig. 4b and c, Table 7, the pseudo second-order kinetic model for  $\text{Fe}^{3+}$  adsorption mechanism over LL502 showed excellent linearity with a high correlation coefficient ( $R^2=0.9999$ ) while a pseudo first-order kinetic model was not close to 1, probably

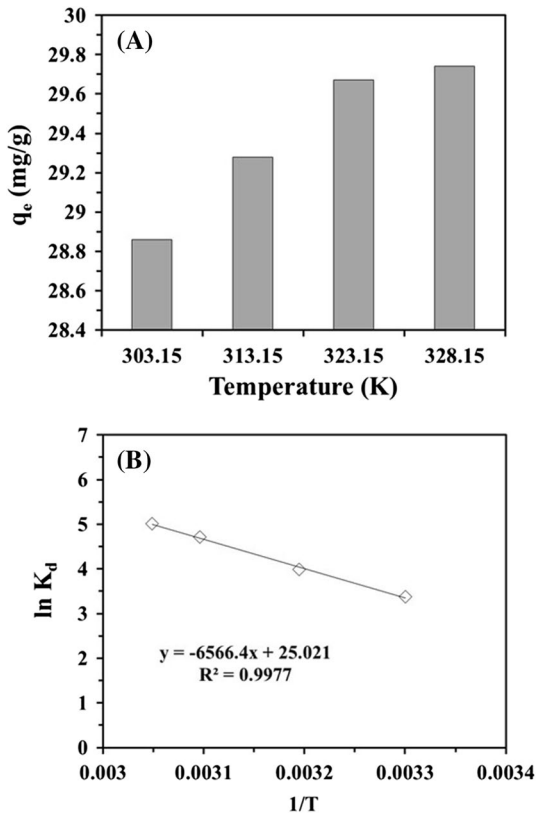
due to occurrence of very fast Fe<sup>3+</sup> adsorption. In addition, the calculated  $q_e$  values (29.15 mg/g) were also very close to  $q_e$  values (28.32 mg/g) derived from the experimental result, confirming that this selected model had high accuracy.

In order to get more information on performance of LL502, its adsorption thermodynamic was studied at temperatures of 303.15–328.15 K. As shown in Fig. 5, an increase in the adsorption temperature could promote the adsorption efficiency of Fe<sup>3+</sup> on LL502, suggesting the nature of the endothermic adsorption process. In addition, higher temperature could enhance a better diffusion rate of Fe<sup>3+</sup> across the external boundary layer and in the internal pores of the LL502 structure, as well as decrease the viscosity of the mixture solution. The parameters of adsorption thermodynamics such as standard enthalpy ( $\Delta H$ , kJ/mol), standard entropy ( $\Delta S$ , J/mol K) and Gibbs standard free energy ( $\Delta G$ , kJ/mol) at different temperatures were also determined using the following Eqs. (12)–(15) [25]:

$$k_d = \frac{C_0 - C_e}{C_e}, \tag{12}$$

$$\Delta G = -RT \ln K_d, \tag{13}$$

**Fig. 5** **a** Effect of temperature and **b** thermodynamics of Fe<sup>3+</sup> adsorption onto LL502. Relative combined expanded uncertainty tSE is  $< \pm 0.03$  mg/g (0.95 level of confidence). The initial concentration of adsorbate/ $C_0$  of Fe<sup>3+</sup> = 120 mg/L, 25 mL, adsorbent = 0.10 g, time/ $t$  = 60 min and temperature ( $T$ ) = 303.15–328.15 K



$$\Delta G = \Delta H - T\Delta S, \quad (14)$$

$$\ln K_d = \frac{\Delta S}{R} - \frac{\Delta H}{RT}, \quad (15)$$

where  $C_e$  is the equilibrium concentration of the  $\text{Fe}^{3+}$  (mg/L),  $C_0$  is the initial concentration of  $\text{Fe}^{3+}$  (mg/L),  $R$  is the universal gas constant (8.314 J/mol K),  $T$  is the absolute temperature (K) and  $K_d$  is the distribution coefficient.

As shown in Fig. 5b and Table 7,  $\Delta G$  obtained from  $\text{Fe}^{3+}$  adsorption onto LL502 at different temperatures was a negative value at the range between  $-13.65$  and  $-8.5$  kJ/mol. This change in free energy could be attributed to the spontaneous nature of the physisorption process [26]. It should be noted that physisorption was in the range of  $\Delta G$  between  $-20$  and  $0$  kJ/mol, while the chemisorption the range was in between  $-80$  and  $-400$  kJ/mol. Here,  $\Delta G$  value was obviously decreased to some extent with an increasing of adsorption temperature, which was in good agreement with results in Fig. 5a. Moreover,  $\Delta H$  and  $\Delta S$  also presented positive values, indicating endothermic adsorption of  $\text{Fe}^{3+}$  under irreversible and randomness processes [27]. The physisorption process was well confirmed with  $\Delta H < 100$  kJ/mol, which corresponded with the result derived from the Dubinin–Radushkevich isotherm. For comparisons of the adsorption performance with previous literature, as shown in Table 8, higher  $\text{Fe}^{3+}$  adsorption capacities were obtained using LL502 based on  $q_{e \max}$  than other previously developed adsorbents. From these results, LL502 could be considered as a promising low-cost/efficient adsorbent for selective removal of metal cation from wastewater in industrial processes.

## Conclusions

In summary, the surface of all adsorbents, except ACC, clearly appeared as a negative charge ( $\text{pH}_{\text{pzc}} > \text{pH}$  of mixture solution), resulting in a high ability for  $\text{Fe}^{3+}$  adsorption. LL502 was found to be the best feedstock for production of activated carbon and removal of  $\text{Fe}^{3+}$ . It also presented high efficiency for iron removal up to 98% from ground/surface water. The water quality index in ground/surface water after treatment process could be well improved, compared with the water quality standard.

**Table 8** Comparison of adsorption capacities of  $\text{Fe}^{3+}$  with various adsorbents

Adsorbent	Adsorption capacity of $\text{Fe}^{3+}$ (mg/g)	References
$\text{Fe}_3\text{O}_4@\text{mSiO}_2\text{-NH}_2$	20.66	[23]
Hazelnut hull	13.59	[28]
Natural clay	12.86	[29]
Acid-activated clay	19.25	
Granular activated carbon	4.91	[30]
Amberlite IR-120H	8.01	
LL502	32.89	This work

The maximum adsorption capacities of Fe<sup>3+</sup> using LL502 obtained from the monolayer adsorption process via the Langmuir isotherm ( $R^2 > 0.99$ ) were 32.89 mg/g. The adsorption behavior and data on monolayer-physorption with a rapid adsorption process were also verified by Dubinin–Radushkevich and pseudo-second order kinetic models. Moreover, thermodynamic results indicated that the adsorption process of Fe<sup>3+</sup> onto a LL502 surface was endothermic and spontaneous in nature.

**Acknowledgements** The authors wish to acknowledge Department of Chemistry, Faculty of Science, Rangsit University for supporting all instruments and chemicals.

## References

1. C. Dalai, R. Jha, V.R. Desai, *Aquat. Procedia* **4**, 1126 (2015)
2. H. Jeong, H. Kim, T. Jang, *Water* **169**, 1 (2016)
3. D. Vollprecht, L. Krois, K.P. Sedlazeck, P. Müller, R. Mischitz, T. Olbrich, R. Pomberger, J. Cleaner Prod. **208**, 1409 (2019)
4. K. Sasaki, Y. Hayashi, K. Toshiyuki, B. Guo, *Chemosphere* **207**, 139 (2018)
5. L. Cai, L. Cui, B. Lin, J. Zhang, Z. Huang, *J. Cleaner Prod.* **202**, 759 (2018)
6. N. Chitpong, S.M. Husson, *Sep. Purif. Technol.* **179**, 94 (2017)
7. J. Valentín-Reyes, R.B. García-Reyes, A. García-González, E. Soto-Regalado, F. Cerino-Córdova, *J. Environ. Manage.* **236**, 815 (2019)
8. P. Maneechakr, S. Karnjanakom, *J. Chem. Thermodyn.* **106**, 104 (2017)
9. P. Maneechakr, P. Chaturatphattha, S. Karnjanakom, *Res. Chem. Intermed.* **44**, 7135 (2018)
10. W. Phairuang, M. Hata, M. Furuuchi, *J. Environ. Sci.* **52**, 85 (2017)
11. W. Shen, Z. Li, Y. Liu, *Chem. Eng.* **1**, 27 (2008)
12. R.B. Fidel, D.A. Laird, M.L. Thompson, *J. Environ. Qual.* **42**, 1771 (2013)
13. Q. Shi, A. Terracciano, Y. Zhao, C. Wei, C. Christodoulatos, X. Meng, *Sci. Total Environ.* **648**, 176 (2019)
14. Y. Gao, S. Xu, Q. Yue, Y. Wu, B. Gao, *J. Taiwan Inst. Chem. Eng.* **61**, 327 (2016)
15. J.P. Chen, S. Wu, *Langmuir* **20**, 2233 (2004)
16. L. Huang, J. Kong, W. Wang, C. Zhang, S. Niu, B. Gao, *Desalination* **286**, 268 (2012)
17. M.H. Marzbali, M. Esmaili, H. Abolghasemi, M.H. Marzbali, *Process Saf. Environ. Prot.* **102**, 700 (2016)
18. M. Kılıç, E. Apaydın-Varol, A.E. Pütün, *Appl. Surf. Sci.* **261**, 247 (2012)
19. Z. Sun, Y. Yu, S. Pang, D. Du, *Appl. Surf. Sci.* **284**, 100 (2013)
20. H. Shayesteh, A. Rahbar-Kelishami, R. Norouzbeigi, *J. Mol. Liq.* **221**, 1 (2016)
21. M. Ghaedi, A. Ansari, F. Bahari, A.M. Ghaedi, A. Vafaei, *Spectrochim. Acta, Part A* **137**, 1004 (2015)
22. P. Roy, N.K. Mondal, K. Das, *J. Environ. Chem. Eng.* **2**, 585 (2014)
23. C. Meng, W. Zhikun, L. Qiang, L. Chunling, S. Shuangqing, H. Songqing, *J. Hazard. Mater.* **341**, 198 (2018)
24. H.D. Choi, W.S. Jung, J.M. Cho, B.G. Ryu, J.S. Yang, K. Baek, *J. Hazard. Mater.* **166**, 642 (2009)
25. S. Karnjanakom, P. Maneechakr, *J. Mol. Struct.* **1186**, 80 (2019)
26. H. Saygılı, F. Güzel, *Ecotoxicol. Environ. Saf.* **131**, 22 (2016)
27. M.N. Sepehr, A. Amrane, K.A. Karimaian, M. Zarrabi, H.R. Ghaffari, *J. Taiwan Inst. Chem. Eng.* **45**, 635 (2014)
28. A. Sheibani, M. Shishebor, H. Alaei, *Int. J. Ind. Chem.* **3**, 1 (2012)
29. K. Leila, C. M. Luisa, S. N. Soaad, B. Mohamed, *Sep. Sci. Technol.*
30. M.E. Goher, A.M. Hassan, I.A. Abdel-Moniem, A.H. Fahmy, M.H. Abdo, S.M. El-sayed, *Egypt. J. Aquat. Res.* **41**, 155 (2015)

**Publisher's Note** Springer Nature remains neutral with regard to jurisdictional claims in published maps and institutional affiliations.